Article type : Original Manuscript

Intraspecific variation in feeding mechanics and bite force in durophagous stingrays

Matthew A. Kolmann, PhD*
Friday Harbor Laboratories, University of Washington
620 University Rd, Friday Harbor, WA, 98250
Email: kolmann@uw.edu
Phone: 360-320-8194

R. Dean Grubbs, PhD
Florida State University Coastal and Marine Laboratory
3618 Coastal Highway 98, St. Teresa, FL 32358, USA
Email: dgrubbs@bio.fsu.edu
Phone: 850-697-2067
Fax: 850-697-3822

Daniel R. Huber, PhD
Department of Biology, University of Tampa
401 W. Kennedy Boulevard, Tampa, FL 33606, USA
Email: dhuber@ut.edu
Phone: 813-257-3995
Fax: 813-258-7496

Robert Fisher, MSc
Marine Advisory Services, Virginia Institute of Marine Science
1208 Greate Rd, Gloucester Point, VA 23062, USA
Email: rfisher@vims.edu
Phone: 804-684-7168

Nathan R. Lovejoy. PhD
Department of Biological Science, University of Toronto Scarborough
1265 Military Trail, Toronto, ON, M1C 1A4, Canada
Email: lovejoy@utsc.utoronto.ca
Phone: 416-208-4823
Fax: 416-287-7642

Gregory M. Erickson, PhD
Department of Biological Science, Florida State University
319 Stadium Drive, Tallahassee, FL 36303, USA
Email: gerickson@bio.fsu.edu
Phone: 850-645-4991

Abstract

Animal performance is tightly linked to morphological function, whereby changes in size and performance can influence niche dynamics over ontogeny. To understand how growth affects feeding performance, we examined how bite force over ontogeny differed between two populations of durophagous stingrays, *Rhinoptera bonasus* (from the Chesapeake Bay and the Florida Gulf Coast, USA). Cownose stingrays from the Chesapeake Bay specialize on mollusks, whereas Gulf of Mexico stingrays are omnivorous, feeding on a variety of benthic invertebrates. Increases in jaw adductor size resulted in positive bite force allometry across ontogeny in both stingray populations. However, scaling patterns between muscle units differed between the populations, with more drastic increases in bite force over ontogeny in populations feeding on more robust prey. Mechanical testing of the fracture forces of prey suggests that juvenile bivalves are particularly vulnerable to predation by either stingray population. However, Gulf coast stingrays exhibit lower bite forces across ontogeny compared to Chesapeake rays.

Chesapeake Bay rays are born larger, further exaggerating the performance disparity between these populations. Although these animals generate considerable bite forces, their ability to comminute bivalves at marketable sizes is doubtful.

Key Words: bite force, durophagy, ecomorphology, Myliobatidae, shellfish declines, trophic cascade, stingray, *Rhinoptera bonasus*

Introduction

Changes in animal size and shape underlie shifts in performance and resource use over ontogeny (Verwaijen, van Damme, and Herrel, 2002; Vincent et al., 2007; Gignac and Erickson, 2015). When competing with sympatric taxa, species specialize on some nuance of a shared resource to stave off competition, particularly when formerly abundant resources become scarce (Liem, 1980). While increases in predator size expand access to larger prey items and potentially more diverse prey through isometric increases in performance (particularly with regards to bite force), juvenile predators may circumvent size constraints via allometric performance trajectories (Herrel and Gibb, 2006; Anderson, McBrayer, and Herrel, 2008; Habegger *et al.*, 2012). Allometric performance gains allow juveniles to access the energy resources required for rapid growth, thereby also reducing predation risk and conspecific competition (Arnold, 1983; Werner and Gilliam, 1984). Increased feeding performance is presumably selected for early in ontogeny, when younger animals are under considerable selective pressure to perform in a manner similar to adults, with which they may co-occur and even compete (Erickson, Lappin, and Vliet, 2003).

Durophagous taxa feed on prey with exoskeletons that are particularly tough, stiff, or hard and can serve as a viable study system for relating ontogeny of performance to prey characteristics. Although ancestrally possessing compliant cartilaginous skeletons, several lineages of chondrichthyan fishes have evolved highly mineralized jaws enabling them to act as durophagous predators (Summers, 2000; Dean and Summers, 2006). Among these taxa are myliobatid stingrays like cownose rays (*Rhinoptera bonasus*; Mitchill, 1815), which occur in the southeastern United States, with one population inhabiting coastal waters from Virginia to Florida and the other, the Gulf of Mexico (Schwartz, 1990; Aschliman, 2014; Fig. 1). Cownose rays from the Chesapeake Bay region are typically larger (female median size at maturity, 860 mm; Fisher, Call, and Grubbs, 2013) than Gulf of Mexico individuals and primarily consume shelled prey such as bivalves. Those from the Gulf of Mexico on the other hand are smaller (female median size at maturity, 653 mm; Neer and Thompson, 2005; Fig. 1) and primarily consume smaller bivalve taxa and softer-bodied benthic invertebrates, such as cumaceans and amphipods (Collins *et al.*, 2007; Fisher, 2010;

Ajemian and Powers, 2012; Fisher *et al.*, 2013; Fig. 1). Given the occurrence of resource-based plasticity in the feeding mechanisms of fishes (Turingan, Wainwright, and Hensley, 1995; Hernandez and Motta, 1997; Wintzer and Motta, 2005), differences in the diet of cownose ray populations may be echoed by ecomorphological specialization, whereby rays feeding on more robust prey are expected to be more robust, thereby maximizing feeding performance (i.e. bite force).

Here we examine whether feeding performance is greater in durophagous Chesapeake Bay cownose rays compared to more omnivorous rays from the Gulf of Mexico, using a biomechanical model that estimates bite forces across ontogeny for both populations. These anatomical models have been shown to accurately predict bite force generation in live cownose rays (Kolmann *et al.*, 2015a). We hypothesize that bite force performance will be greater in stingrays from Chesapeake Bay. We also expect that differences in muscle scaling and greater size-at-parturition of these Chesapeake Bay rays allows greater bite force generation in Chesapeake rays relative to their Gulf of Mexico relatives. We examined the ecological ramifications of alternate feeding performance in these two predator populations by quantifying the rupture behavior of several kinds of mollusk prey. We demonstrate that Chesapeake Bay rays can crush a larger size range of prey, as well as a greater diversity of mollusks earlier in ontogeny, than more omnivorous rays from the Gulf of Mexico.

Methodology

Specimen Collection

Rhinoptera bonasus specimens were obtained through fishery-independent surveys of two regions, the Gulf Coast of Florida and Chesapeake Bay, Virginia. Gulf of Mexico (n = 27) animals were collected by National Marine Fisheries Service (NMFS) - Panama City Laboratory, Florida Fish and Wildlife Commission - Charlotte Harbor and Eastpoint Labs, and by the authors (RDG, MK) during NMFS GulfSPAN surveys of elasmobranch diversity, between Panama City in the northwestern panhandle region of Florida and south to Charlotte Harbor. Stingrays from Virginia (n = 21) were collected by the authors (RDG, RF) during the Virginia Institute of Marine Science and ChesMMAP surveys. Disk width (DW, in cm), as a metric of body size, was recorded along with geographic location, sex, and maturity. All animals were sacrificed in accordance with Institutional Animal Care and Use Committee guidelines (protocol #: 1118; RDG) at Florida State University or by the guidelines of each respective agency.

Bivalve species were collected using a variety of methods throughout Florida and Chesapeake Bay. Oysters (*Crassostrea virginica*, n = 22) were obtained manually from pilings at the Florida State University Coastal and Marine Laboratory, collected from VIMS shellfish surveys, or commercially purchased (Mineral Springs Seafood Company, Panacea, FL). Coquina clams (*Donax variabilis*, n = 45)

were collected manually from high-energy beaches with a shovel and sieve, between Alligator Point and Carabelle Beach, FL. Larger *C. virginica*, hard clams (*Mercenaria mercenaria*), and other bivalves (*Mya arenaria, Ensis minor, Mytilus edulis,* and *Ostrea ariakensis*) were obtained from the Chesapeake Bay region, VA.

Bite-Force Modeling

The theoretical bite-force modeling for *Rhinoptera bonasus* followed Kolmann *et al.* (2015a). In brief, the relative origin and insertion of each muscle, the position of the jaw joint, and the bite points were measured relative to a three-dimensional coordinate system with its origin at the anterior-most, medial tip of the palatoquadrate cartilage using digital calipers. In order to determine the lever geometry of the feeding apparatus, as well as the relative direction and magnitude of the in-forces generated by each muscle, the relative positions of all anatomical points were determined by measuring their distances from the *X, Y,* and *Z* planes intersecting at the origin (Huber *et al.*, 2005, 2006, 2008). Muscle identity of *R. bonasus* follows Kolmann *et al.* (2014) (Fig. 2).

Muscle force output scales in proportion to muscle fiber cross-sectional areas (Powell *et al.*, 1984). It was estimated, in parallel-fibered muscles in the present study, by sectioning the muscle through its center of mass, perpendicular to the fiber angle direction, and then digitally photographing the cross section (EOS Rebel, Canon Inc., Lake Success, New York). For muscles with pennate-fibered morphology, physiological cross-sectional area was estimated using to the following equation:

$$\text{Physiological CSA} = \text{muscle mass muscle density X } \cos\emptyset \text{ fiber length}$$

(*Ø represents the insertion angle of the muscle fibers onto the central tendon of the muscle*)

Muscle CSA, fiber length, and fiber angle and length were measured from the digital photographs using ImageJ v. 1.40 (National Institute of Health, Bethesda, MD). Theoretical maximum tetanic tension (P_o) was determined by multiplying the muscle CSA (either anatomical or physiological) by the specific tension (T_s) for elasmobranch red muscle (14.9 Nm^{-2} – Lou, Curtin, and Woledge, 2002):

$$P_o = CSA * T_s$$

In-lever (L_i) distances were calculated using the insertion of each muscle on the lower jaw and the position of the jaw joint using the 3D coordinate system. A resultant in-lever distance was determined by using a weighted average of all the muscle in-levers, with weighting conditional on the overall force

contribution of each muscle. Out-lever (L_O) distances were based on the positions of the medial bite point in comparison to the jaw joint. Mechanical advantage (MA) at the medial bite point was calculated by dividing the resultant in-lever by its out-lever distance.

A static equilibrium model was used to calculate the summation of the bending moments generated by the jaw adducting musculature about the jaw joints, and used to estimate theoretical maximum medial bite forces (BF_{med}) (Huber *et al.*, 2005). The static equilibrium of all the forces acting on the lower jaw (F_{LJ}) is represented by the following equation:

$$\Sigma F_{LJ} = F_{JR} + F_{AMMe} + F_{SB} + F_{AMLa} + F_{AMMa} + F_{AMD} + F_{AMLi} + F_B = 0$$

(F_{JR} *is the joint reaction force [which balances bite force and allows summation to* 0], F_B *is the bite force occurring for a given prey item at one of the bite points, while* F_{AMMe}, F_{SB}, F_{AMLa}, F_{AMMa}, F_{AMD}, F_{AMLi} *are the adductor muscle forces acting upon the lower jaw*)

Equilibrium models were run for medial biting scenarios only as this is the primary location (according to wear on the tooth modules) where prey is first grasped and then ruptured.

Prey Rupture Forces

We examined how rupture forces scaled over ontogeny for *Donax variabilis* and *Crassostrea virginica*, for which we had ontogenetic series. Given the limited size sample for other bivalve taxa in our study, we examined qualitatively how rupture forces differed between prey bivalves that may be be consumed by either *Rhinoptera* population. There is some overlap in diets between Gulf of Mexico and Chesapeake populations of cownose rays; both taxa consume veneroid clams such as *Donax* (*D. variabilis*) and *Ensis* (*E. minor*) as well as mytilids like *Mytilus edulis* and *Geukensia demissa* (Ajemian and Powers, 2012). However, Chesapeake cownose rays have historically consumed larger soft-shell clams such as *Mya arenaria* (Smith and Merriner, 1985). *Crossostrea virginica* and *Mercenaria mercenaria* make up a small component of the diet of cownose rays in Chesapeake Bay (Smith and Merriner, 1985, Fisher 2010), but have not been confirmed in the diet of cownose rays from the Gulf of Mexico (Collins *et al.*, 2007; Ajemian and Powers, 2012).

Bivalve specimens were measured for shell depth: the greatest dorso-ventral distance perpendicular to the umbo. Shellfish were subjected to axial compression tests using two different a mechanical loading frame systems: (A) an Material Testing Station (model 312.31, MTS Corp., Eden Prairie, MN, USA) with a 2500N load cell (model 661.19e-01, MTS Corp.) for smaller specimens of *Crassostrea virginica* and *Donax variabilis;* or (B) a 100 Kip Enerpac (Actuant Corp., Menomonee Falls, WI, USA) manual hydraulic pump and jack system, connected to a 25 kN load cell (model 661.20b-01,

MTS Corp.) for larger oysters (*C. virginica*, *C. ariakensis*), mussels, (*Mytilus edulis*), soft clams (*Mya arenaria*), razor clams (*Ensis minor*), and hard clams (*Mercenaria mercenaria*). All compression tests were performed on live or recently deceased shellfish. All bivalve specimens were crushed along their dorso-ventral axis with a constant loading rate of $0.5 mms^{-1}$ (Pfaller, Gignac, and Erickson, 2011).

In scenario (A), shellfish were crushed using the actual, preserved jaws from an adult cownose ray (72 cm DW), while in scenario (B), shellfish were crushed between two steel plates. In scenario (A), the jaw was embedded upside-down in a mold of mixed fiberglass fibers and Elite© Stone dental molding cement (Zhermack Inc. River Edge NJ). Axial displacement of the loading frame pushes against a load cell, which was affixed with a steel peg. The peg contacted a subsequent steel roller, resting in the wing process of the Meckel's cartilage of the lower jaw, allowing jaw closure to maintain a natural configuration. The average natural gape height for each pair of jaws was not exceeded during testing on shellfish (Fisher, Call, and Grubbs, 2011). To determine if the two methods of testing, for those species for which we have overlap in sampling, shell depth was regressed against shell failure force. The residuals of this regression were compared with a Welch's t-test to determine if there were significant differences in the mean for either method.

Statistical Analysis

Muscle forces, masses and CSAs, as well as lever distances, and pennate-fibered muscle fiber lengths and angles were $\log_{10}$-transformed and linearly regressed using reduced major axis regression (RMA) against $\log_{10}$-transformed body size (disk width). We tested whether our metric for body size, disk width, scaled is an appropriate or comparable metric (with body mass) for scaling analyses, using OLS regression to confirm an isometric relationship between log-transformed disk width and body mass ($n = 984$). Mechanical advantage ratios and muscle fiber angles were left untransformed as these values are dimensionless (Pfaller *et al.*, 2011). Scaling relationships between these variables with respect to body size were determined by comparing the regression slopes versus the expected isometric slope for that given variable (mechanical advantage and fiber angles = 0; lever distances = 1; areas and forces = 2, muscle masses = 3). Confidence intervals generated around RMA slopes were compared to the expected isometric slope for each variable in order to determine positive or negative performance allometry, or isometry. Reduced-major axis regression was also used to determine the scaling relationships between shell size and shell rupture forces. For descriptive purposes, we used an isometric slope of 2 to compare the scaling relationship between shell depth and shellfish rupture forces. Reduced major axis regressions, including slope, elevation, and shift comparisons of regression models were performed using the *lmodel2* and *smatr* packages.

Kolmann and colleagues (2015a), measured bite forces from live cownose rays and found them to be approximately twice the estimated values for bite forces determined from feeding anatomy. For comparisons of bite force to shell rupture forces, we used anatomically-determined bite force values as our minimum estimates of feeding performance, and then doubled these values to obtain an absolute maximum estimate of bite force at a given ecologically-relevant life history stage (neonates, young-of-the-year, and mature adults). Mean disk width at critical life stages (neonates, year 1, and population-level median size at maturity) in *Rhinoptera* were gathered from the literature for the Gulf Coast of Mexico (Neer and Thompson, 2005; Poulakis, 2013) and Chesapeake Bay (Fisher *et al.*, 2013) populations. The maximum forces required to fracture mollusks of known dimensions were then used to generate regression (OLS) equations from which either shell depth or shell rupture forces could be extrapolated (Hernandez and Motta, 1997). By inputting estimated stingray bite forces into these equations, and solving for shell size we determined the size range of shellfish vulnerable to predation.

The lack of an entire size series for bivalve prey (*Mya sp, Mercenaria sp, Mytilus sp, Ostrea ariakensis*, and *Ensis sp*) other than *Donax* sp and *Crassostrea sp.*precluded us from running further statistical analyses to determine what life stages these mollusks would be vulnerable to predation. Therefore, we present rupture forces for these taxa qualitatively in comparison to *D. sp* and *C. sp*. All statistical analyses were implemented using R (version 2.15.0; www.theRproject.org).

Results

Biomechanical Scaling

Scaling relationships between body size (DW) and biomechanical and physiological variables for cownose rays from the Gulf of Mexico are detailed in Kolmann *et al.* (2015a). Regressions of log-transformed body mass (kg) against disk width (cm) show tight correlation, increasingly isometrically throughout the size range of cownose rays (slope = 3.25, r^2 = 0.9898). Similar to findings from Kolmann et al. (2015), the mass of the main jaw adductor, the adductor mandibulae major (AMMa) in Chesapeake Bay stingrays is both the largest jaw-closing muscle as well as the greatest contributor to overall muscular in-force (Table S1). The AMMa in rays from the Chesapeake Bay produces 45.7% of the overall muscle force (54.7% in rays from Florida), followed by the suborbitalis (11.7%; 13.9% in Florida rays), adductor mandibulae lateralis (AMLa – 9.1%; 12.7% in Florida rays), AM lingualis (AMLi – 6.8%; 9.4% in Florida rays), AM deep (5.7%; 7.3% in Florida rays), and AM medialis (1.26%; 1.7% in Florida rays) (Table 1). All jaw adductor masses scale with positive allometry relative to disk width (Table S1), while all jaw adductor cross-sectional areas also increased with positive allometry (Table S1). Jaw adductor forces scaled with positive allometry in Chesapeake Bay and Florida stingrays; the adductor mandibulae major (slope = 3.06; 3.76 in Florida rays), followed by the suborbitalis (slope = 3.56; 4.08 in Florida

rays), adductor mandibulae lateralis (slope = 3.01; 4.04 in Florida rays), AM lingualis (slope = 2.64; 4.02 in Florida rays), AM deep (slope = 2.96; 3.66 in Florida rays), and AM medialis (slope = 3.56; 4.38 in Florida rays) (Table S1). However, in Chesapeake Bay stingrays both the fiber angle (slope = -1.53) and fiber length (slope = 1.31) of the AM major scaled isometrically with respect to disk width over the ontogeny (Table 2).

In Chesapeake Bay stingrays lever distances with respect to body size scaled with positive allometry (Table 2). The medial out-lever scaled with positive allometry (slope = 1.13; 0.97 in Florida rays) and the resultant in-lever (weighted by muscle contribution to overall bite force) also scaled with positive allometry with respect to disk width (slope = 1.21; 1.00 in Florida rays; Fig. 3). Given that the out-lever as well as the in-lever scaled with positive allometry, mechanical advantage scaled isometrically (medial MA slope = 0.26; -0.36 in Florida rays; Table 2). Gulf of Mexico rays also showed isometric scaling of mechanical advantage, but due to comparable, isometric scaling across all lever distances (Kolmann *et al.*, 2015a). Medial bite forces scaled with positive allometry with respect to disk width through ontogeny (slope = 2.42; 2.36 in Florida rays; Table 2).

Bite forces were higher in rays collected from the Chesapeake Bay at all stages of their ontogeny than rays from the Gulf of Mexico (Fig. 4). This higher performance was due to both an elevational change and shift in the regression line of Chesapeake over Gulf coast rays: Virginia cownose are both larger in size and have higher performance than Florida cownose rays (elevation: Wald statistic = 8.389; $p = 0.003$; shift: Wald statistic = 15.9; $p < 0.006$). However, regression slopes between Chesapeake and Gulf Coast stingrays were indistinguishable ($p = 0.285$; LRT = 1.139).

Prey Rupture Testing

Welch's t-test results show no significant differences between our two failure testing methods (t = 1.2324, p = 0.2254). In coquina clams (*D. variabilis*), rupture forces scaled isometrically (slope = 2.36; CI: 1.971-2.838) when compared to shell depth ($p < 0.01$; $r^2 = 0.626$). Rupture forces in eastern oysters (*C. virginica*) scaled with negative allometry (slope = 0.63; CI: 0.573-0.694) with regards to shell depth ($p < 0.01$; $r^2 = 0.841$) (Fig. 5). Linear regressions of rupture force (N) on shell depth were used for comparisons between cownose ray bite forces and prey rupture forces (Fig. 5).

Gulf neonate cownose rays (mean DW ~ 30cm; Poulakis, 2013) are predicted to have the capacity of consuming *Donax* sp. clams approximately 0.6-0.9 cm shell depth (Fig. 5) using their average bite force of 29.5 N. Chesapeake Bay neonate cownose rays (mean DW ~ 42cm; Fisher *et al.*, 2013) could theoretically consume *Donax*. sp. clams of 0.6-1.5 cm shell depth with bite forces exceeding 81.7 N. Year 1 Gulf of Mexico (~47 cm DW) and Chesapeake Bay cownose rays (~63cm DW) could potentially consume the rest of the size series of *Donax. sp* clams represented in this data set (Fig. 5). Neonate Gulf

rays (mean DW ~ 35cm) could consume up to 0.42-0.78cm shell depth for eastern oysters (Fig. 5). Chesapeake Bay cownose rays (median DW ~ 40cm) could theoretically consume eastern oysters of up to 0.53-1.1 cm shell depth (Fig. 5). Year 1 Gulf of Mexico rays (~47 cm DW) could rupture up to 0.69-1.1 cm shell depth for eastern oysters. Year 1 Chesapeake Bay rays (~47 cm DW) could rupture 1.04-2.18 cm shell depth oysters. Mature Gulf cownose rays (~70cm DW) could theoretically rupture 1.2-2.18 cm shell depth eastern oysters. Mature Chesapeake Bay cownose rays (~85cm DW) could theoretically rupture 1.5-2.18 cm shell depth eastern oysters. Both cownose ray populations have comparable adult-level performance, i.e. both are capable of feeding on the entire size range of their respective potential prey, by year two of their development (Fig. 5).

Discussion

This study is the first to address interspecific differences in feeding performance between elasmobranch populations. All muscle CSAs, masses, and forces scaled with positive allometry over the development of cownose rays from Chesapeake Bay. This stands in contrast to patterns recovered from Gulf of Mexico stingrays, in which only three of six jaw muscles showed positive, allometric growth in muscle CSA and only two of six jaw muscles showed positive allometry of force generation (Kolmann *et al.*, 2015a). In addition, Chesapeake Bay rays are born larger, by approximately 10-12cm (Poulakis, 2013; Fisher *et al.*, 2013) leading to an absolute difference in initial performance due to size alone. These findings support the weight of literature regarding vertebrate feeding systems, which overwhelmingly demonstrate that trophic partitioning between related taxa is mediated by absolute differences in size in many taxa, and by alternate modes of performance scaling in many dietary specialists (Anderson *et al.*, 2008). Both populations of cownose rays follow the latter pattern, but with larger size at parturition in Chesapeake Bay rays further contributing to overall higher performance early in ontogeny.

Overall, rays from the western Chesapeake Bay showed higher bite force performance values at all sizes than cownose rays from the Gulf of Mexico. These higher bite forces presumably allow Chesapeake Bay rays to access less-robust bivalve taxa (e.g. *Donax* sp.) within their first year of growth, compared to rays from the Gulf of Mexico (Figures. 5 & 6). However, after year one, Gulf coast cownose rays are predicted to be able to consume the entire size range of *Donax sp*, making these rays potential predators even at small sizes (Fig. 6). Although we are not able to statistically determine the relationship between prey rupture forces for some bivalve prey with respect to stingray feeding performance, Figure 6 illustrates how some harder mollusks common to the Chesapeake Bay region (*Mya sp.* and *Mytilus sp.*) are well within neonate levels of feeding performance for cownose rays from this area. Timely access to an expanded size range and diversity of mollusks increases the probability that these stingrays can successfully consume readily available prey. While within-species variation in size at birth can represent

a means of coping with higher predation pressure, shorter growing seasons, and a migratory life history strategy, we also find that larger neonate sizes confer higher feeding performance (and perhaps even foraging, by reducing prey-handling times; Fisher et al., 2011).

Differences in muscle size explain the disparity in feeding performance between the two cownose stingray populations, whereas the scaling of the jaw lever mechanics are comparable. In rays from the Chesapeake Bay, positive allometry of both in-levers and out-levers cancelled out such that the overall mechanical advantages show an isometric pattern through ontogeny. Gulf of Mexico rays also exhibit isometric mechanical advantage, although this on the contrary is the product of isometric growth in both the jaw adducting in-lever and out-levers. These findings suggest the presence of strong constraints on the remodeling ability of the jaw musculoskeletal module, leaving muscle physiology, architecture, and growth as the primary means driving ontogenetic changes in feeding performance. The lack of a tongue, or other means of fine-scale prey manipulation might be limiting to these animals making movement of prey to an ideal position to maximize force transmittance in these animals with rays relatively akinetic jaws relative to other stingrays (Dean, Wilga, and Summers, 2005; Mulvany and Motta, 2014; Kolmann *et al.*, 2014, 2016; but see Sasko *et al.*, 2006).

These findings are another example of equifinality in the feeding apparatus of myliobatid stingrays and other vertebrates (Young, Haselkorn, and Badyaev, 2007; Kolmann *et al.*, 2015b). Despite differences regarding the relative positions of muscle insertions (in-lever), jaw joint (fulcrum), and occlusal surface (out-lever), jaw mechanical advantage remains functionally equivalent between both stingray taxa. Whereas Kolmann *et al.* (2015a) postulated that conservative growth patterns of jaw leverage in Gulf of Mexico *Rhinoptera* were due to constraints on remodeling jaw cartilage, our findings suggest that this scenario is more complex. Maintenance of biomechanically advantageous leverage performance throughout ontogeny, rather than leverage augmentation, seems to be a motif for rhinopterines as opposed to other durophagous chondrichthyans and other vertebrates in general (Huber *et al.*, 2008; Kolmann & Huber, 2009; Pfaller *et al.*, 2011). We hypothesize that this could be necessary to ensure constancy of force transmittance along the entire occlusal surface, allowing prey to be crushed across the broad dental battery.

Cownose rays, like their distant cousins the California bat ray (*Myliobatis californica*) have been implicated in commercially-harvested shellfish declines such as oysters (Smith and Merriner, 1985; Gray, Mulligan, and Hannah, 1997; Myers *et al.*, 2007). However, dietary studies analyzing gut contents for cownose rays show that bivalves make up a negligible component of their overall diet (Collins *et al.*, 2007; Ajemian and Powers, 2012). In fact, California bat rays were shown to prey overwhelmingly on one of the Pacific oysters' primary predators – crabs of the genus *Cancer* (Gray *et al.*, 1997). Recent reanalysis of the findings of Myers *et al.* (2017) by Grubbs *et al.* (2016) found that declines in large

coastal sharks did not coincide with purported increases in cownose ray populations, nor did cownose ray abundances coincide with shellfish declines. Furthermore, Grubbs *et al*. (2016) found little evidence for 'explosive' population growth in *Rhinoptera* in Chesapeake Bay. Fisher *et al.* (2011) showed that even in conditions where *Rhinoptera* were forced to consume oysters of various sizes, probability of predation dropped precipitously at shell depths greater than 2.3 cm for adults, and for juveniles at 0.8 cm shell depth (Fisher *et al*., 2011). Our findings support Fisher (2011) in that adult cownose rays are not capable of crushing oysters much larger than 2.0cm in shell depth, which on average exceed the 550-650 N bite forces large rays can generate. In fact, the rupture forces for most of the commercially valuable bivalves which cownose rays have allegedly consumed fall far outside the maximum estimated performance for mature adult rays (Fig. 6). Bivalves within these ranges of shell depth would be considered of marketable size (7-8 cm), suggesting that cownose rays are incapable of consuming shellfish at their most marketable size classes, although juvenile shellfish are still at risk (Fisher *et al.*, 2011).

Acknowledgments

We thank C. Bedore, D. Bethea, J. Christofferson, L. Harris, J. Pfeiffenberger, and M. Pfleger for assistance with specimen collection. M. Daniels, B. Henderson, C. Koenig, D. Overlin and D. Tinsley who built aquaria and facilitated animal transport. M. Dobrovetsky and D. Kay assisted with data collection and dissection. P. Gignac and A. Watanabe provided advice during data collection and revisions. Two anonymous reviewers provided valuable feedback on the first draft of this manuscript. Funding for this project was provided by a Florida State University Coastal and Marine Laboratory Graduate Research Grant and Ontario Trillium Scholarship to M.A.K., FSUCML start-up funding to R.D.G., a University of Tampa Research Grant to D.R.H., National Oceanic and Atmospheric Administration funding to R.F., and a Natural Sciences and Engineering Research Council of Canada Discovery Grant to N.R.L.

References

Ajemian, MJ, & Powers, SP. (2012). Habitat-specific feeding by cownose rays (*Rhinoptera bonasus*) of the northern Gulf of Mexico. *Env. Biol. Fish*, 95, 79-97.

Anderson, RA, McBrayer, LD, & Herrel, A. (2008). Bite force in vertebrates: opportunities and caveats for use of a nonpareil whole-animal performance measure. *Biol. J. Linnean. Soc*. 93: 709-720.

Arnold, SJ. (1983). Morphology, performance, and fitness. *Amer. Zool*, 23, 347-361.

Aschliman, N.C., 2014. Interrelationships of the durophagous stingrays (Batoidea: Myliobatidae). *Env. Biol. Fish*. 97, 967-979.

Clifton, KB, & Motta, PJ. (1998). Feeding morphology, diet, and ecomorphological relationships among five Caribbean labrids (Teleostei, Labridae). *Copeia*, 1998, 953-966.

Collins, AB, Heupel, MR, Hueter, RE, & Motta PJ. (2007). Hard prey specialists or opportunistic generalists? An examination of the diet of the cownose ray, *Rhinoptera bonasus*. *J. Mar. Freshw. Res.* 58, 135–144.

Dean, MN, Wilga, CD, & Summers, A.P. (2005). Eating without hands or tongue: specialization, elaboration and the evolution of prey processing mechanisms in cartilaginous fishes. *Biol Lett*, 1, 357-361.

Dean, MN, Summers, AP. (2006). Mineralized cartilage in the skeleton of chondrichthyan fishes. *Zoology*, 109, 164-168.

Erickson, GM, Lappin, AK, & Vliet, KA. (2003). The ontogeny of bite-force performance in American alligator (*Alligator mississippiensis*). *J. Zool*, 260, 317-327.

Fisher, R.A. (2010). Life history, trophic ecology, & prey handling by the cownose ray, *Rhinoptera bonasus*, from Chesapeake Bay. Report to NOAA (Grant # 713031).

Fisher, RA, Call, GC, & Grubbs, RD. (2011). Cownose ray (*Rhinoptera bonasus*) predation relative to bivalve ontogeny. *J. Shellfish Res*, 30, 187-196.

Fisher, RA, Call, GC, & Grubbs, RD. (2013). Age, growth, and reproductive biology of cownose rays in Chesapeake Bay. *Mar. Coast. Fish*, 5, 224-235.

Gignac, PM, & Erickson, GM. (2015). Ontogenetic changes in dental form and tooth pressures facilitate developmental niche shifts in American alligators. *J. Zool*, 295, 132-142.

Gray, AE, Mulligan, TJ, & Hannah, RW. (1997). Food habits, occurrence and population structure of the bat ray, *Myliobatis californica*, in Humboldt Bay, California. *Env. Biol. Fish*, 49, 227–238.

Grubbs, RD, Carlson, JK, Romine, JG, Curtis, TH, McElroy, WD, McCandless, CT, Cotton, CF, & Musick, JA. (2016). Critical assessment and ramifications of a purported marine trophic cascade. *Scientific Reports*, 6.

Habegger, ML, Motta, PJ, Huber, D.R, & Dean, MN. (2012). Feeding biomechanics and theoretical calculations of bite force in bull sharks (*Carcharhinus leucas*) during ontogeny. *J. Zool*, 115, 354-364.

Herrel, A, & Gibb, AC. (2006). Ontogeny of performance in vertebrates. *Physiol. Biochem. Zool* , 79, 1-6.

Hernandez, LP, & Motta, PJ. (1997). Trophic consequences of differential performance: ontogeny of oral jaw-crushing performance in the sheepshead, *Archosargus probatocephalus* (Teleostei, Sparidae). *J. Zool*, 243, 737-756.

Huber, DR, Weggelaar, CL, & Motta, PJ. (2006). Scaling of bite force in the blacktip shark *Carcharhinus limbatus*. *J. Zool*, 109, 109-119.

Huber, DR, Dean, MN, & Summers, AP. (2008). Hard prey, soft jaws and the ontogeny of feeding mechanics in the spotted ratfish, *Hydrolagus colliei*. *J. R. Soc. Interface*, 5, 941–952.

Kolmann, MA, & Huber, DR. (2009). Scaling of feeding biomechanics in the horn shark *Heterodontus francisci*: Ontogenetic constraints on durophagy. *J. Zool*, 112, 351–361.

Kolmann MA, Huber DR, Dean MN, & Grubbs RD. (2014). Myological variability in a decoupled skeletal system: batoid cranial anatomy. *J.Morphol*, 275, 862-81.

Kolmann, MA, Huber, DR, Motta, PJ, & Grubbs, RD. (2015). Feeding biomechanics of the cownose ray, *Rhinoptera bonasus*, over ontogeny. *J. Anat*, 227, 341-351.

Kolmann, MA, Crofts, SB, Dean, MN, Summers, AP, & Lovejoy, NR. (2015). Morphology does not predict performance: jaw curvature and prey crushing in durophagous stingrays. *J. Exp. Biol*, 218, 3941-3949

Lou, F, Curtin, NA, & Woledge, RC. (2002). Isometric and isovelocity contractile performance of red muscle fibers from the dogfish *Scyliorhinus canicula*. *J. Exp. Biol*, 205, 1585-1595.

Liem, KF. (1980). Adaptive significance of intra-and interspecific differences in the feeding repertoires of cichlid fishes. *Amer. Zool*., 20, 295-314.

Mulvany S & Motta PJ. (2014). Prey capture kinematics in batoids using different prey types: Investigating the role of the cephalic lobes. *J. Exp. Zool: Part A*, 321, 515-530.

Myers, RA, Baum, JK, Shepherd, TD, Powers, SP, & Peterson, CH. (2007). Cascading effects of the loss of apex predatory sharks from a coastal ocean. *Science*, 315, 1846-1850.

Neer, JA, & Thompson, BA. (2005). Life history of the cownose ray, *Rhinoptera bonasus*, in the northern Gulf of Mexico, with comments on geographic variability in life history traits. *Env. Biol. Fish*, 73, 321-331.

Pfaller, JB, Gignac, PM, & Erickson, GM. (2011). Ontogenetic changes in jaw-muscle architecture facilitate durophagy in the turtle *Sternotherus minor*. *J. Exp. Biol*, 214, 1655-1667.

Poulakis, G.R. (2013). Reproductive biology of the Cownose Ray in the Charlotte Harbor estuarine system, Florida. *Mar. Coast. Fish*, 51, 159-173.

Powell PL, Roy RR, Kanim P, et al. (1984). Predictability of skeletal muscle tension from architectural determinations in guinea pigs. *J. Appl. Physiol*, 57, 1715–1721.

Powers, S.P. & Gaskill, D. (2003). Bay scallop-cownose ray interactions. North Carolina Fishery Resources Grant Program Final Report. [FRG # 03-EP-02]

Sasko, DE, Dean, MN, Motta, PJ, & Hueter, RE. (2006). Prey capture behavior and kinematics of the Atlantic cownose ray, *Rhinoptera bonasus*. *Zoology*, 109, 171-181.

Schwartz, F.J. (1990). Mass migratory congregations and movements of several species of cownose rays, Genus *Rhinoptera*: a world-wide review. *J Elisha Mitchell Scientific Soc*, 106, 10-13.

Smith, JW, & Merriner, JV. (1985). Food habits and feeding behavior of the cownose ray, *Rhinoptera bonasus*, in lower Chesapeake Bay. *Estuaries*, 8, 305–310.

Summers, AP. (2000). Stiffening the stingray skeleton-an investigation of durophagy in myliobatid stingrays (Chondrichthyes, Batoidea, Myliobatidae). *J Morphol*, 243, 113-126.

Turingan, RG, Wainwright, PC, & Hensley, DA. (1995). Interpopulation variation in prey use and feeding biomechanics in Caribbean triggerfishes. *Oecologia*, 102, 296-304.

Verwaijen, D, van Damme, R, & Herrel, A. (2002). Relationships between head size, bite force, prey handling efficiency and diet in two sympatric lacertid lizards. *Funct. Ecol*, 16, 842-850.

Vincent, SE, Moon, BR, Herrel, A, & Kley, NJ. (2007). Are ontogenetic shifts in diet linked to shifts in feeding mechanics? Scaling of the feeding apparatus in banded watersnake *Nerodia fasciata*. *J. Exp. Biol*, 210, 205-2069.

Wintzer, AP, & Motta, PJ. 2005. A comparison of prey capture kinematics in hatchery and wild *Micropterus salmoides floridanus*: effects of ontogeny and experience. *J. Fish Biol*, 67, 409-427.

Werner, EE, & Gilliam, JF. (1984). The ontogenetic niche and species interactions in size-structured populations. *Annu. Rev. Ecol. Evol*, 15, 393-425.

Young, RL, Haselkorn, TS, & Badyaev, AV. (2007). Functional equivalence of morphologies enables morphological and ecological diversity. *Evolution*, 61, 2480-2492.

TABLES

Table 1. Descriptive statistics for jaw muscle variables and contribution to bite force generation in Chesapeake Bay *Rhinoptera bonasus*. AMMe: adductor mandibulae medialis, SB: suborbitalis, AMLa: adductor mandibulae lateralis, AMMa: adductor mandibulae major, AMD: adductor mandibulae deep, AMLi: adductor mandibulae lingualis, CSA: muscle cross-sectional area. Animals are 48-104 cm disk width.

Table 2. Results of reduced-major axis regression scaling analyses of mechanical advantage and bite force with respect to disk width (cm) in the feeding apparatus of Chesapeake Bay *Rhinoptera bonasus* (log Y = b log x +log a). Independent variables scaled against log disk width. Significance level ($\alpha = 0.05$). Confidence interval; CI. LO-med: medial out-lever, LO-lat: lateral out-lever, RLI: in-lever, MA-med: medial advantage, MA-lat: lateral mechanical advantage. For scaling scenarios, I = isometry, P = positive, and N = negative. Animals are 48-104 cm disk width.

FIGURES

Figure 1. Diet and geographic range of two populations of *Rhinoptera bonasus.* (a) Percent of mollusk and crustacean prey by volume of gut content; (b) Geographical range of the two populations – Chesapeake Bay rays (red) and Gulf of Mexico (blue).

Figure 2. Cranial musculature of *Rhinoptera bonasus*. (a) Ventral and (b) Dorsal perspectives of the upper and lower jaws removed from cranium. AMMe: Adductor mandibulae medialis, AMLa: Adductor mandibulae lateralis, AMD: Adductor mandibulae deep, AMLi: Adductor mandibulae lingualis, AMMa: Adductor mandibulae major, SB: Suborbitalis, HYM: Hyomandibular cartilage, LP: Levator palatoquadrati, PQ: Palatoquadrate, MK: Meckel's cartilage.

Figure 3. Scaling of jaw lever distances (cm) and mechanical advantage versus disk width over ontogeny in Chesapeake Bay *Rhinoptera bonasus.* Solid lines, reduced major axis regressions for the data; dashed lines, scaling predictions based on isometric growth set to cross data lines at the mean values of each independent variable. (a) Resultant in-lever distance, (b) medial out-lever distance, (c) Medial mechanical advantage. "P" denotes positive allometry, "N" denotes negative allometry, "I" denotes isometry.

Figure 4. Maximum theoretical bite forces (N) over ontogeny in *Rhinoptera bonasus.* Solid lines, reduced major axis regressions for the data; dashed lines, scaling predictions based on isometric growth set to cross data lines at the mean values of each independent variable. (a) Medial bite force in cownose rays from the Gulf of Mexico, (b) Chesapeake Bay, and (c) both populations combined, Gulf of Mexico rays (circles), Chesapeake Bay rays (triangles). Horizontal dashed line indicates age at parturition. "P" denotes positive allometry, "I" denotes isometry.

Figure 5. Scaling of rupture forces (N) for two ontogenetic series of bivalves. Solid lines, reduced major axis regressions for the data; dashed lines, scaling predictions based on isometric growth set to cross data lines at the mean values of each independent variable. Red colors denote performance data from Chesapeake Bay cownose rays, blue colors are performance data from Gulf of Mexico stingrays. (a) *Donax variabilis,* (b) *Crassostrea virginica*. "P" denotes positive allometry, "N" denotes negative allometry, "I" denotes isometry.

Figure 6. Prey bivalve rupture forces (N). Vertical lines represent the gape height limit of adult *Rhinoptera* from Chesapeake Bay. Dotted line is data from Fisher (2011), showing the probability of predation on mollusks by cownose rays from Chesapeake Bay. Blue shading indicates neonate to yearling bite force performance threshold, green shading indicates sub-adult performance threshold, orange shading indicates adult performance threshold. Prey are *Ostrea ariakensis, Crassostrea virginica, Ensis minor, Mytilus edulis, Mercenaria mercenaria, Mya arenaria,* and *Donax variabilis*.

SUPPLEMENTAL MATERIAL

Table S1. Results of reduced-major axis regression scaling analyses of muscle masses, CSAs, and muscle forces with respect to disk width (cm) in the feeding apparatus of Chesapeake Bay *Rhinoptera bonasus* (log Y = b log x +log a). Independent variables scaled against log disk width. Significance level (α = 0.05). Confidence interval; CI. AMMe: Adductor mandibulae medialis, AMLa: Adductor mandibulae lateralis, AMD: Adductor mandibulae deep, AMLi: Adductor mandibulae lingualis, AMMa: Adductor mandibulae major, SB: Suborbitalis. For scaling scenarios, I = isometry, P = positive allometry, and N = negative allometry.

Figure S1. Jaw adductor muscle mass (g) over ontogeny in Chesapeake Bay *Rhinoptera bonasus.* Solid lines, reduced major axis regressions for the data; dashed lines, scaling predictions based on isometric growth set to cross data lines at the mean values of each independent variable. (a) Suborbitalis muscle masses, (b) adductor mandibulae deep muscle masses, (c) adductor mandibulae major muscle masses, (d) adductor mandibulae medialis muscle masses, (e) adductor mandibulae lingualis muscle masses, (f) adductor mandibulae lateralis muscle masses. “P” denotes positive allometry, “I” denotes isometry.

Figure S2. Jaw adductor muscle cross-sectional areas (cm^2) over ontogeny in Chesapeake Bay *Rhinoptera bonasus.* Solid lines, reduced major axis regressions for the data; dashed lines, scaling predictions based on isometric growth set to cross data lines at the mean values of each independent variable. (a) Suborbitalis muscle CSAs, (b) adductor mandibulae deep muscle CSAs, (c) adductor mandibulae major muscle CSAs, (d) adductor mandibulae medialis muscle CSAs, (e) adductor mandibulae lingualis muscle CSAs, (f) adductor mandibulae lateralis muscle CSAs. “P” denotes positive allometry, “I” denotes isometry.

Figure S3. Jaw adductor muscle forces (N) over ontogeny in Chesapeake Bay *Rhinoptera bonasus.* Solid lines, reduced major axis regressions for the data; dashed lines, scaling predictions based on isometric growth set to cross data lines at the mean values of each independent variable. (a) Suborbitalis muscle forces, (b) adductor mandibulae deep forces masses, (c) adductor mandibulae major muscle forces, (d) adductor mandibulae medialis muscle forces, (e) adductor mandibulae lingualis muscle forces, (f) adductor mandibulae lateralis muscle forces. “P” denotes positive allometry, “I” denotes isometry.

Table 1. Descriptive statistics for musculoskeletal variables and bite force generation in Chesapeake Bay Rhinoptera bonasus

Muscle Division	Mass (g)	CSA (cm^2)	In-Lever (cm)	Muscle Force (N)	Percent Contribution to Bite Force (N)
AMMe	1.62 ± 0.247 0.09-4.00	0.31 ± 0.06 0.05-1.35	3.61 ± 0.18 1.89-5.10	3.69 ± 0.43 0.75-8.64	1.26 ± 0.13 0.85-3.85
SB	8.36 ± 0.181 0.90-20.7	2.277 ± 0.27 0.74-5.15	3.41 ± 0.272 1.83-5.24	27.22 ± 0.751 6.56-60.2	11.7 ± 0.74 6.49-19.31
AMLa	4.184 ± 0.196 0.30-13.0	1.75 ± 0.247 0.18-4.04	3.41 ± 0.247 1.83-5.24	17.84 ± 2.13 3.35-40.74	9.17 ± 0.76 5.61-21.44
AMD	3.415 ± 0.196 0.30-10.0	2.268 ± 1.152 0.30-3.29	1.855 ± 0.152 1.07-3.24	17.17 ± 0.542 4.47-49.02	5.76 ± 0.37 2.99-8.80
AMMa	34.53 ± 0.137 3.80-109.0	9.334 ± 1.175 1.55-24.03	4.001 ± 1.175 1.26-6.67	139.08 ± 5.54 23.03-358.23	45.75 ± 2.43 27.99-76.40
AMLi	7.133 ± 0.29 0.80-21.0	1.355 ± 0.172 0.39-3.67	4.189 ± 0.17 2.03-7.52	20.17 ± 1.08 5.81-54.68	6.81 ± 0.34 4.00-9.85

Values are the mean ± s.e.m.

Table 2. Scaling of mechanical advantage and bite force in Chesapeake Bay Rhinoptera bonasus

Independent variables	r^2	Isometric Slope	Intercept (a)	Slope (b)	CI	p	Scaling Scenario
L_O-med.	0.95	1	-3.34	1.13	1.009-1.259	1.59E-13	P
RL_I	0.87	1	-4.18	1.21	1.016-1.440	8.98E-10	P
MA_{med}	0.01	0	-0.53	0.26	0.166-0.418	0.7218	I
MA_{lat}	0.01	0	2.52	-0.38	-0.597- -0.237	0.7036	I
BF_{med}	0.90	2	-5.00	2.42	2.077-2.830	9.17E-11	P

In-lever and out-lever lengths scaled against disk width. Significance level ($\alpha = 0.05$). Confidence interval; CI.

medial mechanical advantage; L_O-med., Medial bite force (N); BF_{med}, resultant in-lever; RL_I, medial mechanical advantage; MA_{med}, lateral mechanical advantage; MA_{lat}.

For scaling scenarios, I = isometry, P = positive allometry and N = negative allometry.

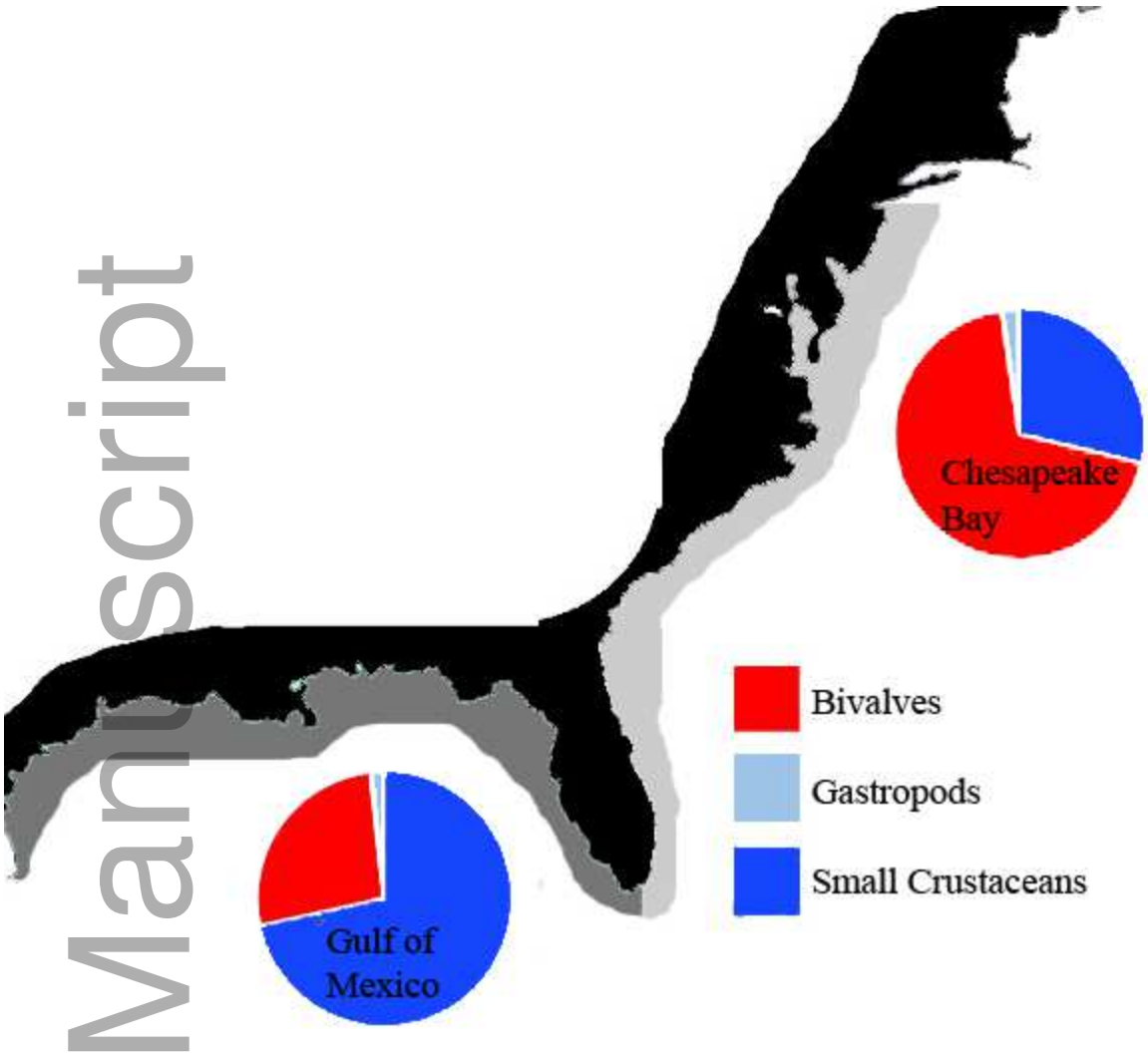

jzo_12530_f1.tif

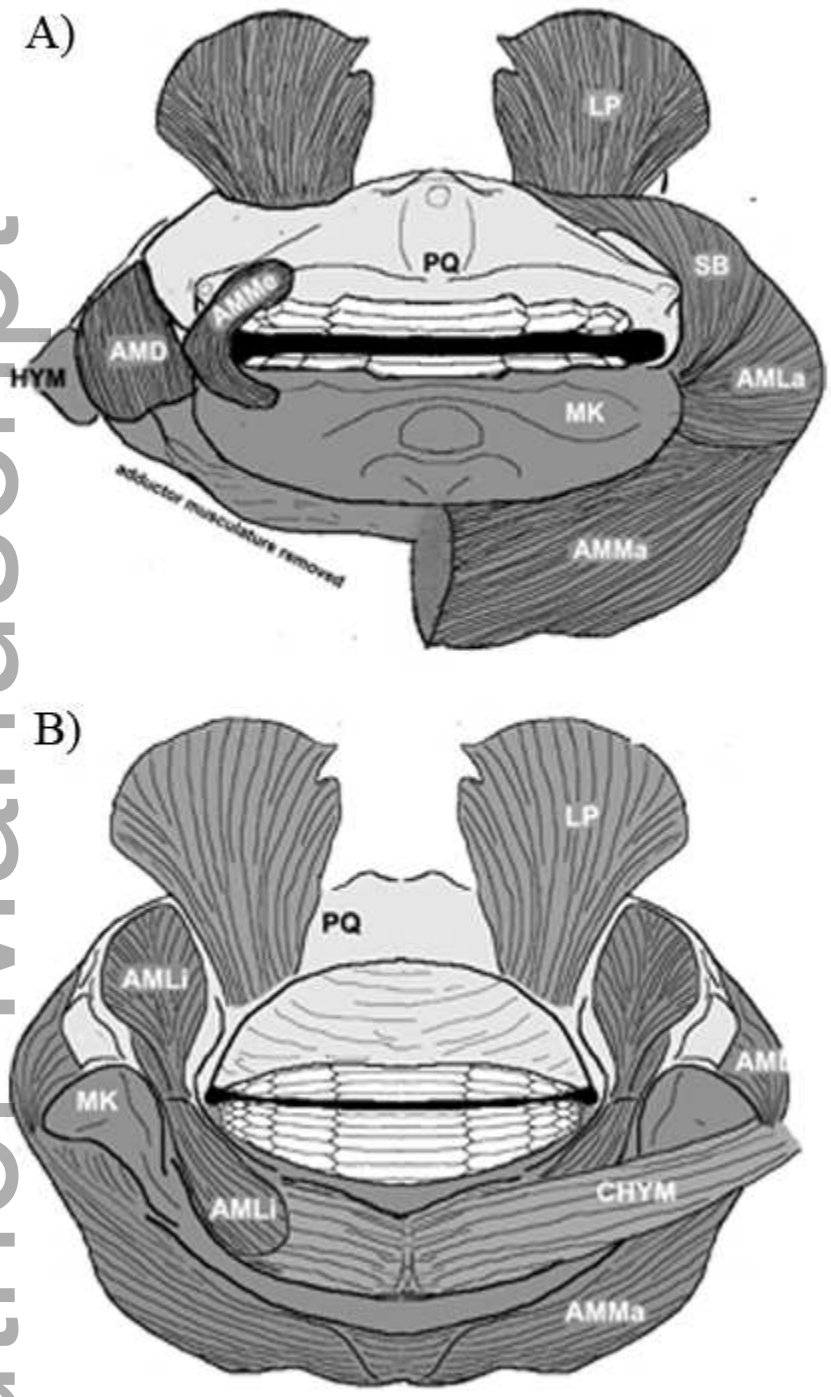

jzo_12530_f2.tif

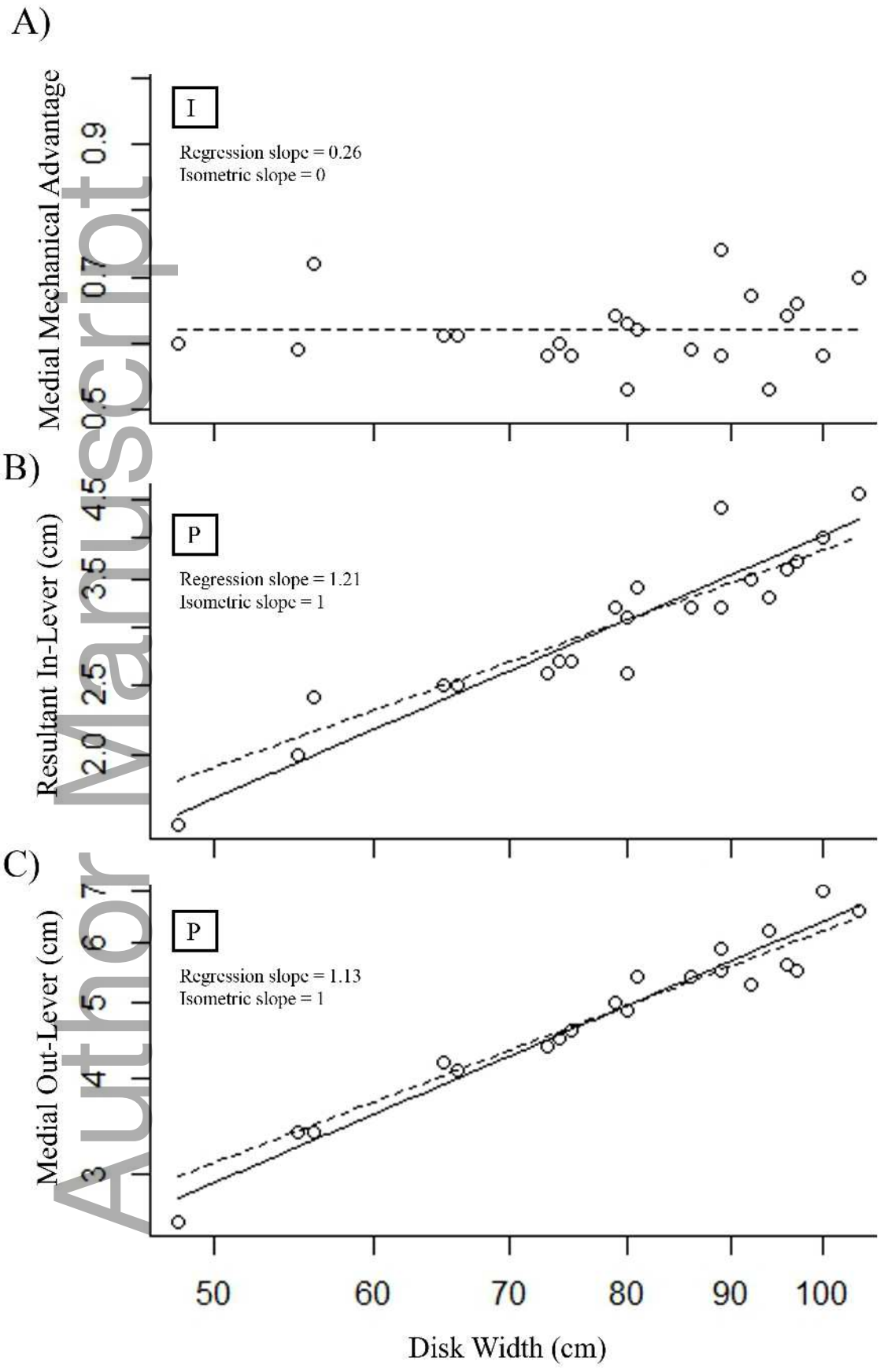

jzo_12530_f3.tif

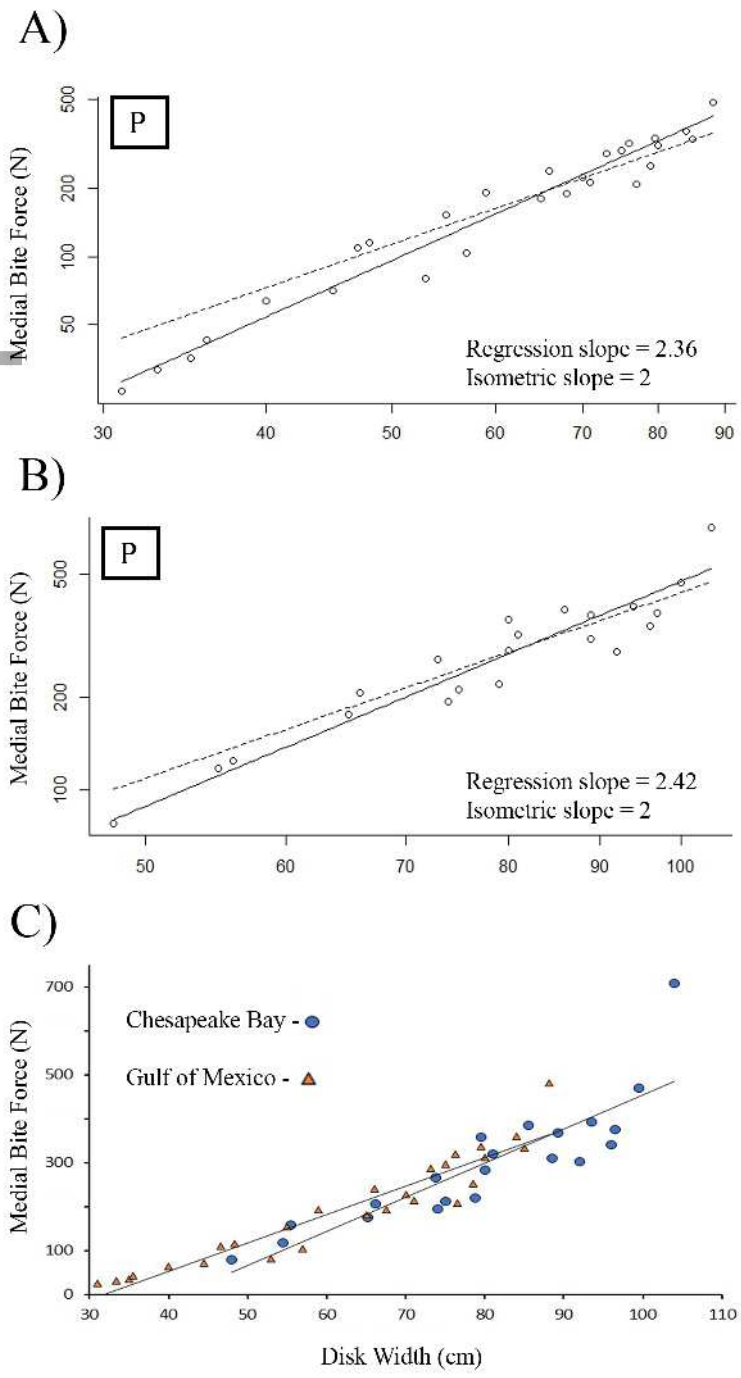

jzo_12530_f4.tif

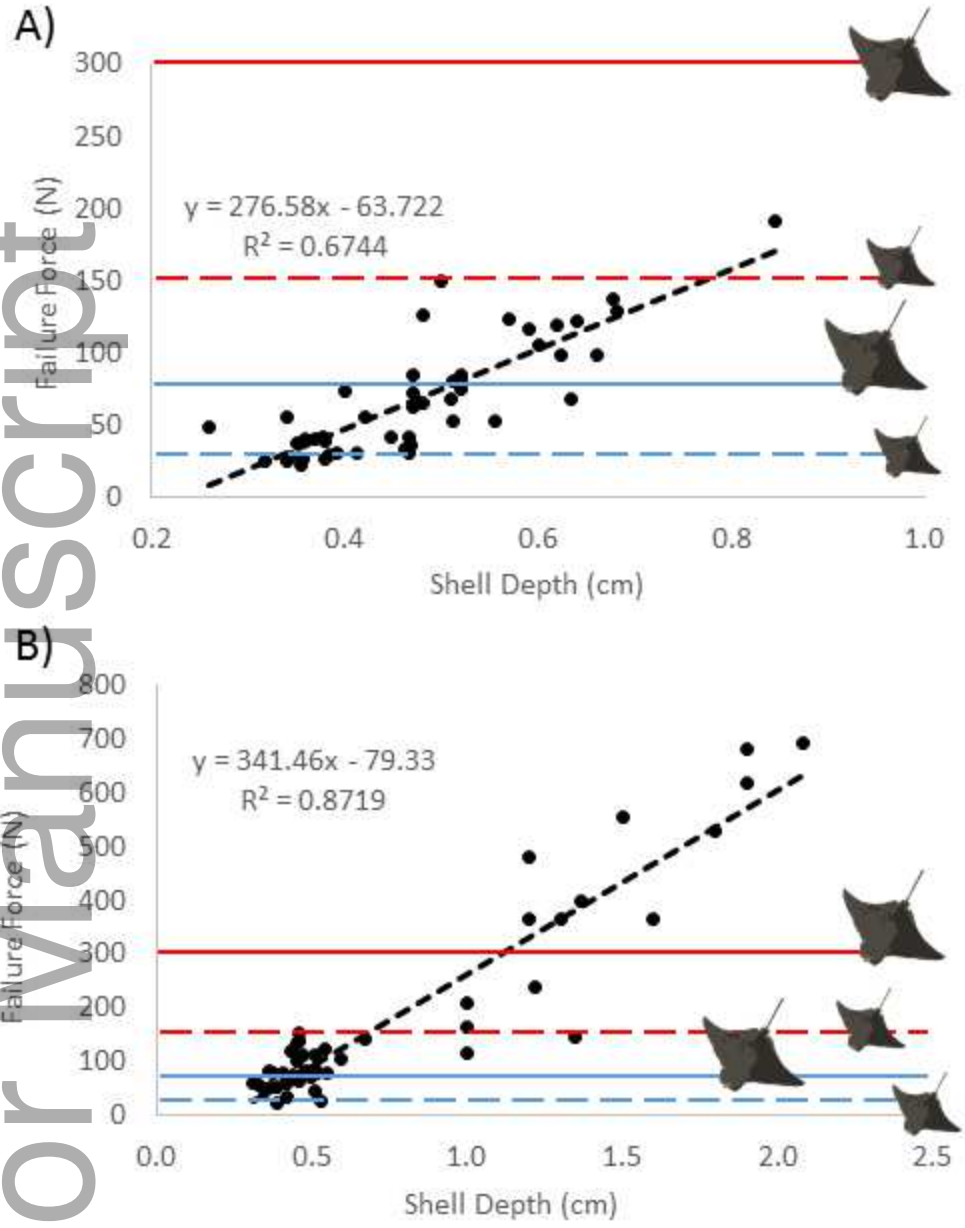

jzo_12530_f5.tif

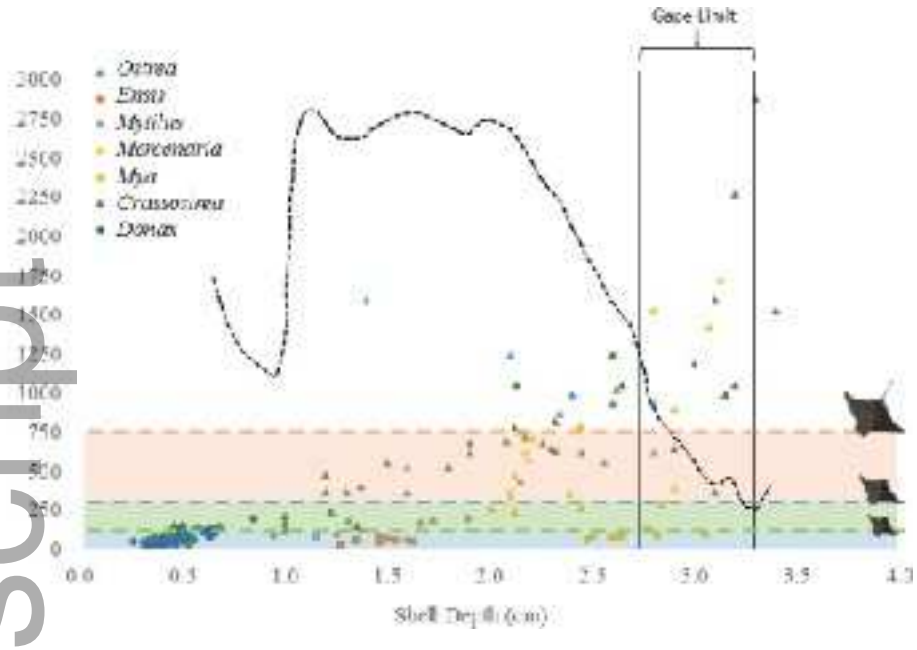

jzo_12530_f6.tif